Available online at www.sciencedirect.com
SCIENCE DIRECT
Polymer 46 (2005) 10897–10907
polymer
www.elsevier.com/locate/polymer

Thermal-induced simultaneous liquid–liquid phase separation and liquid–solid transition in aqueous polyurethane dispersions

Samy A. Madbouly[1], Joshua U. Otaigbe*, Ajaya K. Nanda, Douglas A. Wicks

School of Polymers and High Performance Materials, The University of Southern Mississippi, Hattiesburg, MS 39406, USA

Received 28 April 2005; received in revised form 7 August 2005; accepted 30 August 2005
Available online 23 September 2005

Abstract

Thermal-induced simultaneous phase separation and liquid–solid transition (gelation) in waterborne polyurethane dispersions has been detected morphologically and rheologically. The viscoelastic material functions, such as dynamic shear moduli, G' and G'' complex shear viscosity, η^* and loss tangent, tan δ were found to be very sensitive to the structure evolution during the gelation process and the subsequent formation of a fractal polymer gel. At the onset temperature of the gelation process, an abrupt increase in G', G'' and η^* (several orders of magnitude) was observed during the dynamic temperature ramps (2 °C/min heating-rate) over a wide range of angular frequency. The temperature dependencies of G', G'' and tan δ were found to be frequency independent at the gel-point, T_{gel}, providing a fingerprint for determining T_{gel} of the dispersions. Furthermore, a dramatic increase in zero-shear viscosity, η_0 (v-shape) was observed at $T = T_{gel}$ and found to be in good agreement with the value obtained from the tan δ versus T data. As expected, the time–temperature–superposition principle was found to be only valid for temperatures lower than the T_{gel}; the principle failed at $T \geq 70$ °C. The morphology of the dispersions at 70 °C for 2 h showed for 36, 38 and 40 wt% formation of a network structure having a unique periodicity and phase connectivity. A lower critical solution temperature (LCST) phase diagram was estimated based on the different morphologies of the dispersions. The coexistence of liquid–liquid and liquid–solid transitions at the same temperature range confirmed the complex behavior of the polyurethane dispersions, pointing to the need for a new theory that explicitly takes this special behavior into account.

Keywords: Aqueous polyurethane dispersions; Phase separation and rheology; Fractal gel

1. Introduction

In recent years, waterborne coating systems such as polyurethane dispersions (PUD) have been extensively used due to their health and environmental safety. Rheological properties and gelation of concentrated polyurethane dispersions are little studied and are, therefore, subjects of active research interest due to the industrial importance of these materials. The formation of fractal polymer gel in colloidal dispersions mainly through hydrogen bonds, electrostatic attraction or van der Waals forces allows the immobilization of water within the gel structure [1,2]. Chemical gelation normally take place by gradual branching of linear chains into clusters that are interconnected via covalent bonds to form a three-dimensional polymer network structure [1,2].

A transition of liquid to solid structure (i.e. gelation) with increasing concentration has been reported for hard spheres dispersions [3–6]. This transition is manifested as a non-decaying component of the dynamic structure factor and implies a structural arrest of the crowded suspension [4–6]. Similar phenomenon has been recently reported for weakly attractive soft colloids [7,8]. The gelation process in the soft colloids just mentioned was found to be intrinsically related to the fluid to solid transition, that is manifested as a kinetic arrest, and is driven by the crowding or clusters of particles. This behavior is typical of a wide range of soft materials that lose their ability to flow at high volume fractions [7]. Consequently, it is important to understand and control this transition process and, in more general terms, the different kinds of interactions between the particles during the liquid–solid transition in colloidal dispersions.

Dynamic rheology is a powerful tool for monitoring crosslinking and microstructural changes in a material because it allows properties to be probed under at-rest conditions

* Corresponding author. Tel.: +1 601 266 5596; fax: +1 601 266 5505.
E-mail address: joshua.otaigbe@usm.edu (J.U. Otaigbe).
[1] Permanent Address: Department of Chemistry, Faculty of Science, Cairo University, Orman-Giza 12613, Egypt.

0032-3861/$ - see front matter © 2005 Elsevier Ltd. All rights reserved.
doi:10.1016/j.polymer.2005.08.090

without disruption of the microstructure. In addition, it is also an effective method for studying the curing process of thermosetting polymers and for the examination of the viscoelastic properties and transition temperatures of the cured or coacervated products. The viscoelastic behavior of polymer gels near the sol–gel transition have been studied experimentally [9–16] and theoretically [17–21]. The main emphasis of these studies was to find the relationship between linear viscoelastic properties and the structure of gels at the gel point. The experimental determination and prediction of gelation is important for the processing of crosslinking polymers, while the criticality of the phenomenon and the universality of the properties on the gelation threshold make gelation interesting from a fundamental point of view [22,23]. The formation of polymer gels can be monitored from the time evolution of viscoelastic material functions at the gel point, where the entire network formation process can be divided into two parts separated by the gel point. The gel-point is one of the most important parameter of gelation that is characterized by the appearance in the reactive system of a macromolecule with infinitely large molecular weight. The sol–gel transition point can be determined by a sudden change of a range of physical properties [24]. In theory, the criterion of gel formation is the existence of one long chain running through the whole system. In practice, a sudden loss of flow is the most common and conventional test to determine the sol–gel transition point; because at the gelation point, the viscoelastic properties change abruptly from an initially liquid like state to a solid like state [25–31]. Several models for gelation have been proposed and the most well-known is percolation theory [32,33]. The percolation theory was generalized to predict how the viscoelastic properties, such as dynamic shear moduli and viscosity are expected to scale with time or frequency [34].

In this article the rheological behavior of aqueous PUDs of different compositions will be investigated as functions of temperature and shear frequency. Strong evidence of thermal-induced gelation of PUDs at high PU concentration and in the absence of crosslinking agent will be demonstrated rheologically for the first time to the best of our knowledge. The effects of the gelation process of the PUDs on the dynamic temperature ramps of the viscoelastic material functions, G', G'', $\tan\delta$ and zero-shear viscosity, η_0 will be investigated under different constant shear frequencies. Different theoretical principles such as the time–temperature–superposition and semiempirical equations in the literature will be used to detect formation of fractal gel and to interpret the experimental results. The coexistence of the liquid–liquid transition and the liquid–solid (gelation) transition will be confirmed by studying the morphology of the dispersions.

2. Experimental section

2.1. Materials

Polyester polyol (Desmophen 1019-55), and isophorone diisocyanate (IPDI Desmodur-I) were supplied by Bayer MaterialScience, Pittsburgh, PA. Dimethylol propionic acid (DMPA), dibutyltin dilaurate (DBTDL), 1-methyl pyrrolidinone (NMP), triethyl amine (TEA), hexamethylene diamine (HMDA), diethyl amine (DEA), and tetrahydrofuran (THF) were received from Aldrich Chemical Co. Ethoxylated nonylphenol ammonium sulfate (Abex EP-110, Rhodia Chemicals, Cranbury, NJ) was used as a surfactant. Defoamer (Foamstar-111) was received from Cognis Co., Cincinnati, OH. All the materials were used as received. Table 1 shows the number of moles and molar ratio of the major chemical reagents used.

Table 1
Number of moles and molar ratio of the major chemical reagents used

Recipe	Mole	Molar ratio
Desmophen 1019-55	0.067	1
DMPA	0.103	1.54
IPDI	0.274	4.09

2.2. Prepolymer synthesis

A 250 mL round-bottom, four-necked flask with a mechanical stirrer, thermometer, condenser with nitrogen in/outlet, and a pipette outlet was used as a reactor. The polymerization was carried out in a constant temperature oil bath. Desmophen 1019-55 and DMPA were charged into the dried flask at 70 °C. While stirring, NMP (10 wt% based on total feed) was added and stirring was continued until a homogenized mixture was obtained. Desmodur-I and DBTL were added and stirring was continued for 30 min at this temperature. The mixture was heated to 80 °C for about 3 h to afford an NCO terminated prepolymer. The NCO content during the reaction was determined using a standard dibutylamine back titration method. Upon obtaining a theoretical NCO value, the prepolymers were cooled to 60 °C, and the neutralizing solution, i.e. TEA (DMPA equiv) dissolved in NMP (2 wt%) was added and stirred for 30 min while maintaining the temperature at 60 °C.

2.3. Dispersion and chain extension

Dispersion of PU was accomplished by adding the neutralized prepolymer to the mixture of water and surfactant (4 wt% based on total solid). Agitation was maintained at 750 rpm. After 20 min, 20 wt% solution of HMDA in water was added over a period of 30 min, and chain extension carried out for the next 1 h. At the end, defoamer (Foamstar-111) was added, and stirring continued for 5 min at a speed of 250 rpm. For experiments requiring control of the polymer molecular weight, diethyl amine was included in the chain extension step. In the preparation of all polymers the ratio of isocyanate groups/amine groups (from chain extension/termination) was 1.1/1. Scheme 1 shows schematic reaction steps of prepolymer preparation and chain extension done with urea linkage.

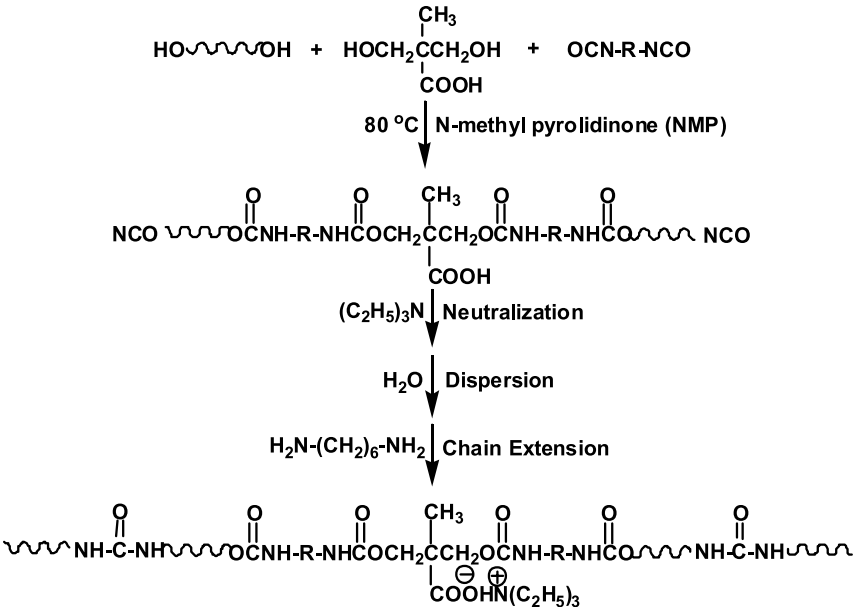

Scheme 1.

2.4. Morphological studies

An Olympus BH2-UMA optical microscope equipped with a Sony CCD camera combined with an optical shearing system (Cambridge Shearing System CSS 450) was utilized in order to analyze the morphological evolution of the dispersions after gelation.

2.5. Rheological measurements

The viscoelastic measurements were done using an advanced Rheometerics Expansion System (ARES, Rheometrics Inc.) equipped with two 25 and 40 mm parallel plates diameter. For very low viscosity samples, we used Physica MCR 501 rheometer with Couette and 25 mm diameter cup. To prevent dehydration of the PUD during testing, a thin layer of low-viscosity silicone oil was applied to the air/sample interface. In this study, the following rheological experiments were performed:

1. Strain sweep at a constant temperature and frequency range of 0.1–100 rad/s to obtain the linear viscoelastic range of the blends.
2. A time sweep at a constant temperature and frequency to obtain steady state and thus, ensure that the measurements were carried out under equilibrium condition.
3. Frequency sweep at a given temperature (10–100 °C) in the linear viscoelastic region (strain amplitude $\leq$10%) to obtain the dynamic shear moduli, i.e. storage shear modulus, G', and loss modulus, G''. The master curves were obtained by horizontal shifts without vertical ones. The zero shear viscosities (η_0) of the blends were also calculated by fitting the η^* versus ω to Cross model [35].

3. Results and discussion

3.1. Rheological gelation behavior of PUDs

The frequency dependence of the PUD complex viscosity at different compositions has been systematically investigated and reported in our previous publication [36]. The viscosity of PUD was dramatically changed as a function of PU concentration. At PU$\leq$40 wt% the viscosity was slightly increased with concentration and nearly independent of frequency. At PU=46 wt% the viscosity increased dramatically (four orders of magnitude) and becomes no longer frequency dependent. The critical concentration at which the viscosity of the dispersions increased dramatically was evaluated based on the Krieger–Dougherty equation [37], and was found to be equal to 0.43 volume fraction [36,37]. Furthermore, the frequency dependence of G' and G'' for

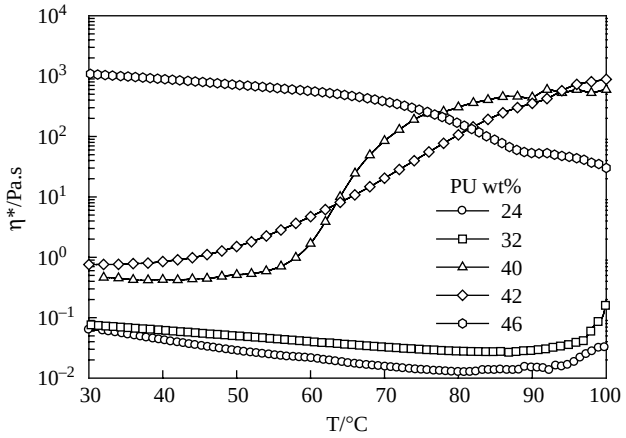

Fig. 1. Temperature dependence of dynamic shear viscosities, η^*, for PUDs of different compositions at 2 °C/min heating-rate and 10 rad/s angular frequency.

the PUDs with varying PU concentrations was also studied. It was found that at PU $\leq$ 40 wt% the PUDs behaved as liquid-like materials (i.e. G' is much lower than G'' and both of them are frequency dependent). At PU = 46 wt% G' and G'' were increased strongly and became frequency independent, indicating the formation of fractal gel. As a continuation of this prior work [36] we now investigate systematically the effect of temperature on the viscoelastic material functions of this important class of dispersion as functions of composition and shear frequency in the present paper.

Fig. 1 demonstrates the temperature dependence of the dynamic viscosity η^* for PUDs of different wt% PU at 2 °C/min heating rate and 10 rad/s angular frequency. As expected, all the samples of different compositions are influenced by increasing the temperature. The viscosity increases strongly at about 95 °C for the samples of 24 and 32 wt% PU. This increase in viscosity is mainly due to the evaporation of water. A dramatic increase (three orders of magnitude) in the viscosity is observed for the sample of 40 wt% PU at around 65 °C. This observation is attributed to the formation of a fractal gel at this temperature. For the sample of 42 wt% PU, the viscosity increases slightly with temperature in the range of $T \leq 50$ °C. At higher temperature range ($90 \geq T \geq 60$ °C) the viscosity increases strongly in a linear manner (Fig. 1). This behavior indicates that the gelation process for the 42 wt% PU sample takes place at lower temperature than that of 40 wt% PU. In addition, the high concentration of 42 wt% PU leads to an increase in the viscosity thereby decreasing the dynamics of the particles and consequently decreasing the probability for the particle–particle interaction. It is essential to mention here that the particle sizes were 73 and 80 nm for 40 and 42 wt% PU, respectively, as previously reported [36]. Therefore, both the hydrodynamic interaction and gelation kinetics should be increased with increasing concentration. Although, the gelation process starts early for 42 wt%, it does not seem to be faster than that of the 40 wt% particularly at high temperature range. This experimental fact may be related to a special morphological attribute that we will consider later in the next section. The pH of the PUDs before and after gelation process were 8.30 and 8.24, respectively. The pH remained constant after gelation, indicating that the triethyl amine was not evaporated during the measurements. Gelation process was also observed for the sample with pH = 10.35 at 65 °C for 2 h in a water bath. At high concentration, such as 46 wt%, the sample turns to a fractal gel at room temperature and the viscosity starts to decrease significantly at around 70 °C. Based on this experimental fact it is apparent that the gelation occurs through flocculation of the dispersed PU particles. As described in Section 2, the PU particles were stabilized through electrostatic and steric repulsions. The electrostatic repulsion was facilitated by the surface charges of PU particles originating from the neutralization of carboxylic acid groups. The steric repulsion is provided by the external surfactant used in preparing the PU dispersions. As the temperature increases, the electric double layer may shrink and the surfactant may be displaced from the PU particle surface, leading to the flocculation of PU particles

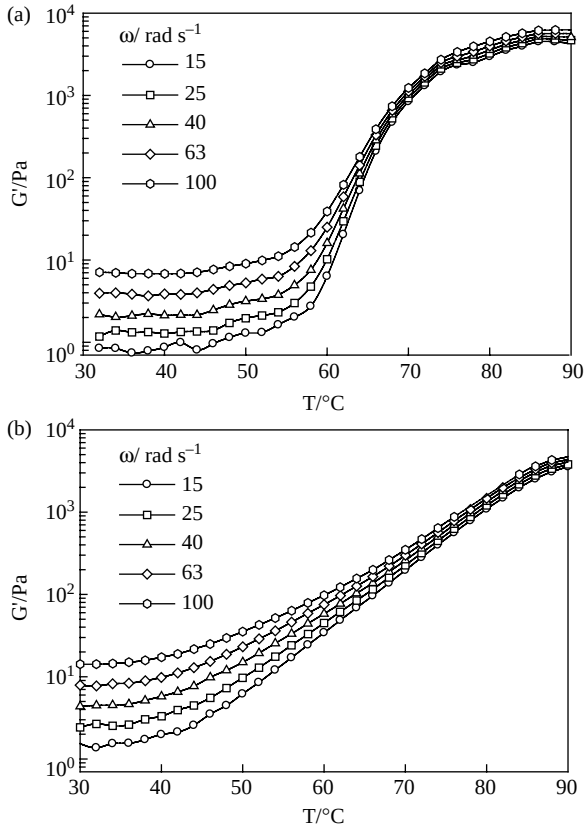

Fig. 2. (a) Temperature dependence of dynamic storage modulus, G', for 40 wt% PU at 2 °C/min heating-rate and different angular frequencies. (b) Temperature dependence of dynamic storage modulus, G', for 42 wt% PU at 2 °C/min heating-rate and different angular frequencies.

in water. This was observed only for PUDs in the high concentration range of PU (PU wt% $\geq$ 36 wt%). In this high PU concentration range the particle sizes are big enough (more than 70 nm) to cause gelation process. However, for PU wt% $\leq$ 34 the gelation process does not take place due to the small particle size (less than 50 nm) and the removal of external surfactant does not induce any flocculation of PU particles in water.

We now describe the effect of thermal induced gelation on the viscoelastic material functions of 40 and 42 wt% PU dispersions as a function of frequency. Fig. 2(a) and (b) demonstrate the temperature dependence of G' at 2 °C/min heating-rate and different constant shear frequencies for the 40 and 42 wt% PU, respectively. For 40 wt% PU, the value of G' is almost constant with increasing temperature at a temperature range lower than the gel temperature (i.e. $T < 60$ °C). A sudden increase in the G' (several orders of magnitude, dependent on the values of applied shear frequency) at about 60 °C (T_{onset}) was observed at all values of frequencies due to the onset of the formation of fractal gel. The magnitude of the elevation in G' increases greatly with increasing temperature due to the evolution of the gelation process and the significant increase in branching (formation of fractal gel). In addition G' is no longer frequency dependent at the high temperature range due to the formation of an equilibrium storage modulus, G'_{eq} which

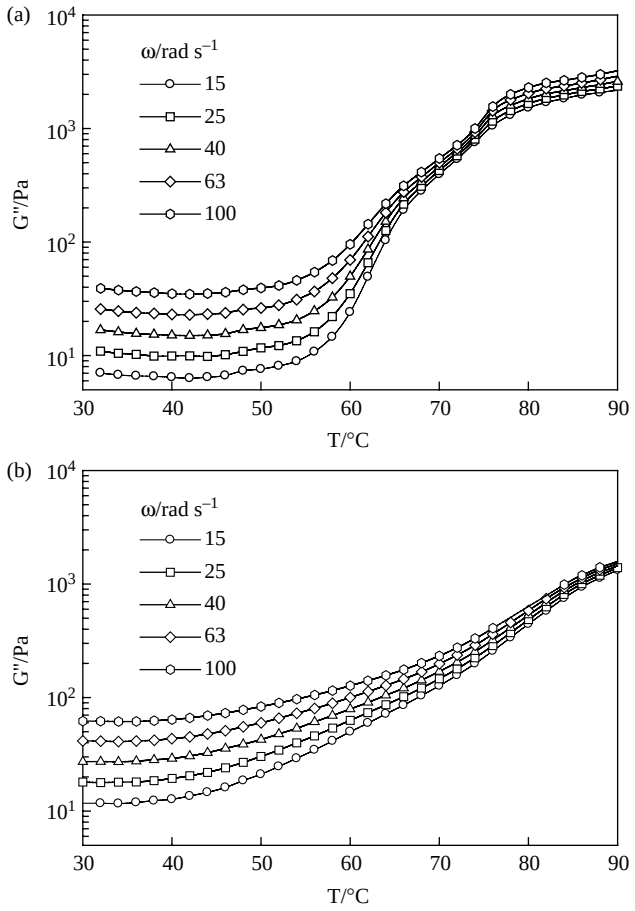

Fig. 3. (a) Temperature dependence of dynamic loss modulus, G'' for 40 wt% PU at 2 °C/min heating-rate and different angular frequencies. (b) Temperature dependence of dynamic loss modulus, G'', for 42 wt% PU at 2 °C/min heating-rate and different angular frequencies.

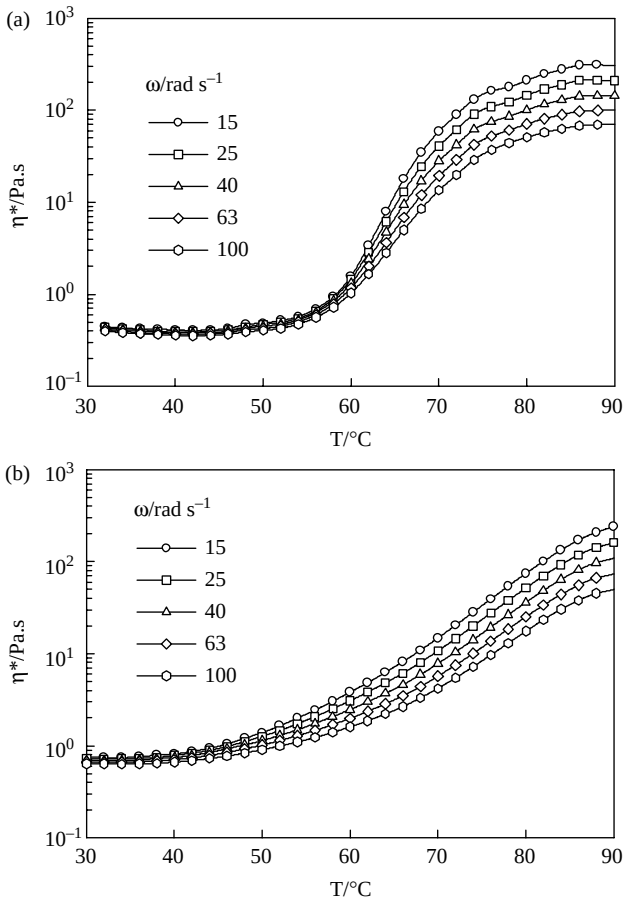

Fig. 4. (a) Temperature dependence of dynamic shear viscosities, η^* for 40 wt% PU at 2 °C/min heating-rate and different angular frequencies. (b) Temperature dependence of dynamic shear viscosities, η^* for 42 wt% PU at 2 °C/min heating-rate and different angular frequencies.

is a typical criterion for the formation of an elastic fractal gel. A similar behavior observed for the 42 wt% PU is shown in Fig. 2(b) with little differences in the value of T_{onset} and the rate (kinetics) of the gelation process. This difference in behavior can be seen very clearly in the different slopes of the G' versus T plots in the temperature range between T_{onset} and the temperature at which $G' \leq G'_{eq}$ (i.e. 65–75 °C for 40% and 60–80 °C for 42 wt% PU).

The dynamic temperature ramps of the loss modulus, G'', for the two samples (40 and 42 wt% PU, respectively) at different constant shear frequencies are shown in Fig. 3(a) and (b). Similar to Fig. 2, G'' abruptly increases at the onset of the gelation process and becomes almost frequency independent at the high temperature range due to the formation of an equilibrium loss modulus G''_{eq}. On the other hand, η^* behaves differently with frequency and temperature for the two different concentrations as shown in Fig. 4(a) and (b). For 40 wt% PU, at $T \leq 60$ °C, η^* is almost constant regardless of frequency and temperature. In fact, the viscosity slightly decreases with frequency and temperature in this temperature range ($T \leq 60$ °C). At $T > 60$ °C, η^* becomes strongly frequency dependent at higher temperature. This different behavior of η^* is attributed to the fact that, at low temperature (i.e. $T < 60$ °C), the PUD exhibits almost frequency independent viscosity behavior over the entire range of frequency. At T_{onset}, the PUD changed from liquid-like to solid-like structure and consequently the η^* becomes frequency dependent as the gelation process evolves into the formation of a fractal polymer gel. For the 42 wt% PU the viscosity of the sample starts to be frequency dependent at about 45 °C. Therefore, the different behavior of η^* with temperature and frequency is not surprising. Details of the frequency dependence of η^* over a wide range of temperature and angular frequency will be considered in the next section.

The gelation temperature, T_{gel}, can be evaluated for this system by two different methods. The first one is from the temperature dependence of the loss tangent, tan δ, at different constant shear frequencies as demonstrated in Fig. 5(a) and (b). The T_{gel} can be obtained from the point at which tan δ is frequency independent and all curves at different constant shear frequencies coincide. Based on this method, the T_{gel} for 40 and 42 wt% PU are 68 and 65 °C, respectively. In the second method, we extract the T_{gel} from the simultaneous temperature dependence of the dynamic shear moduli, G' and G'', as shown in Fig. 6(a) and (b). At temperatures below the T_{onset}, both G' and G'' are frequency dependent and G'' is about one order of

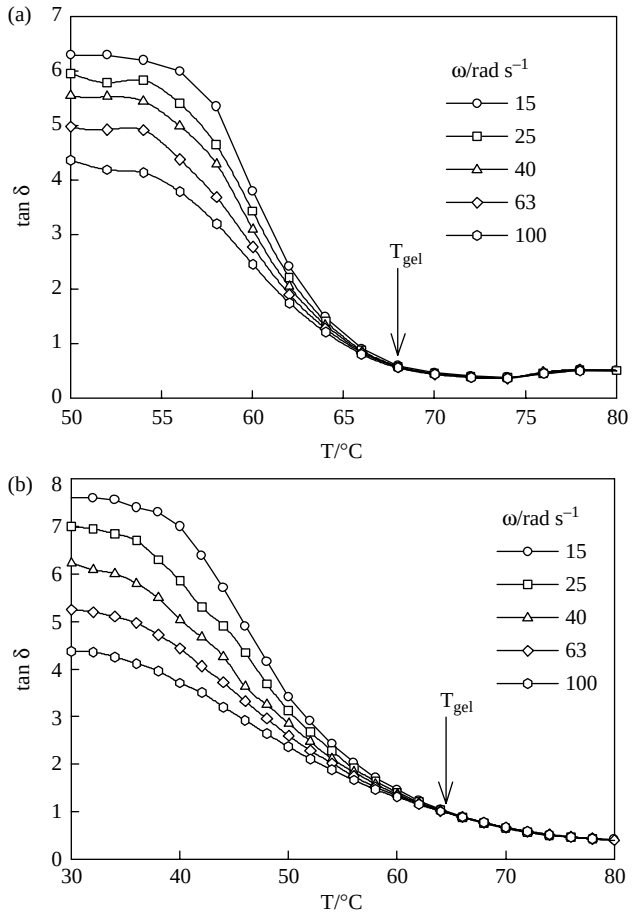

Fig. 5. (a) Temperature dependence of loss tangent, tan δ, for 40 wt% PU at 2 °C/min heating-rate and different angular frequencies. (b) Temperature dependence of loss tangent, tan δ, for 42 wt% PU at 2 °C/min heating-rate and different angular frequencies.

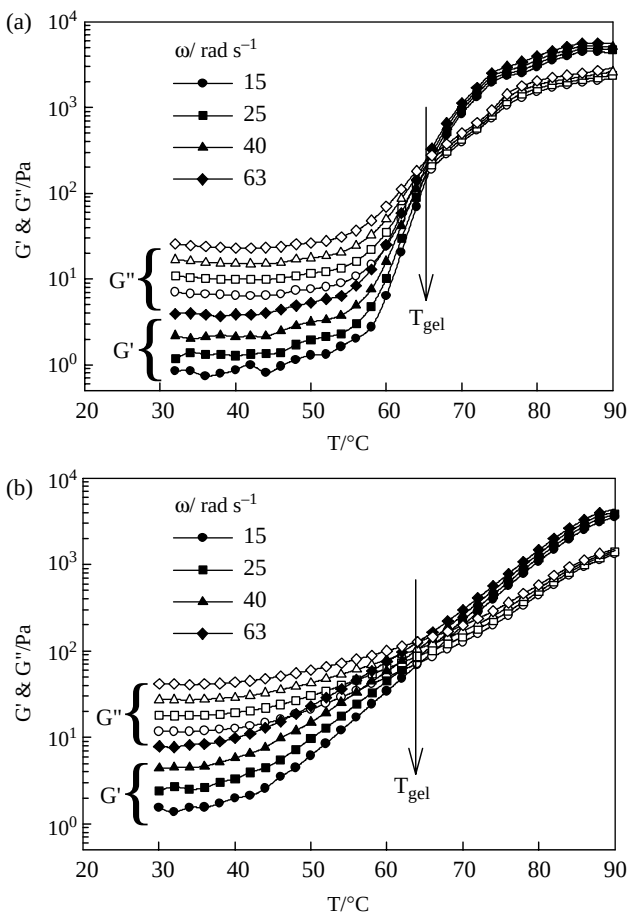

Fig. 6. (a) Temperature ramps of G' and G'' for 40 wt% PU at 2 °C/min heating-rate and different angular frequencies. (b) Temperature ramps of G' and G'' for 42 wt% PU at 2 °C/min heating-rate and different angular frequencies.

magnitude higher than G'. As the T_{onset} is approached, both G' and G'' increase with temperature and coincide at the T_{gel}. At higher temperatures than T_{gel}, the gelation process evolves and G' increases more rapidly than G'' (i.e. G' becomes higher than G'') which is a criterion for the formation of a fractal gel. It must be stated here that the determination of T_{gel} from the crossover of G' and G'' is frequency independent for this system and equal to 68 and 65 °C for 40 and 42 wt% PU samples, respectively. This experimental fact is in good agreement with the values obtained from tan δ versus T plots already discussed. However, it is known for other systems reported in the literature that the crossover of G' and G'' is not a general criterion for determination of T_{gel} due to its high frequency dependence [38,39]. Previously we have reported that the T_{gel} of thermally cross-linked poly(vinyl methyl ether) determined at 100 rad/s was found to be about 20 °C higher than that obtained at 1 rad/s [38]. A similar behavior was recently reported by Zhao et al. [39] who found that the temperature at which the G' and G'' intersect was shear stress and frequency dependent for sol–gel transition of a hybrid gel. Winter et al. [9,10] reported that, when the gelation point cannot be evaluated from the crossover of G' and G'', it could be related to the critical conversion point of crosslinking reaction. At this point both G' and G'' were found to follow a power-law behavior as a function of frequency ($G'' \sim G'' \sim \omega^n$) where n is constant [9,10]. According to the above discussion, it is apparent that, in general, at the T_{gel} the polymer chain branching becomes significant and the fractal polymer network starts to form. At $T > T_{gel}$ the branching proceeds ultimately leading to formation of a fractal gel that is characterized by $G' > G$. In addition, both G' and G'' reach equilibrium values (or become frequency independent). Based on the preceding discussion it appears that, the rheological material parameters (G', G'', η^* and tan δ) of PUDs are very sensitive to the thermal induced gelation process and the formation of a fractal gel network.

Similar behavior to the one just described would be expected for the temperature dependence of zero-shear viscosity, η_0. In order to evaluate the value of η_0 as a function of temperature, measurements of the shear frequency dependence of the complex dynamic viscosity were carried out over a wide range of temperatures below and above T_{gel} (67 °C) for 40 wt% PUD. A typical frequency dependence of η^* at different constant temperatures is shown in Fig. 7. This

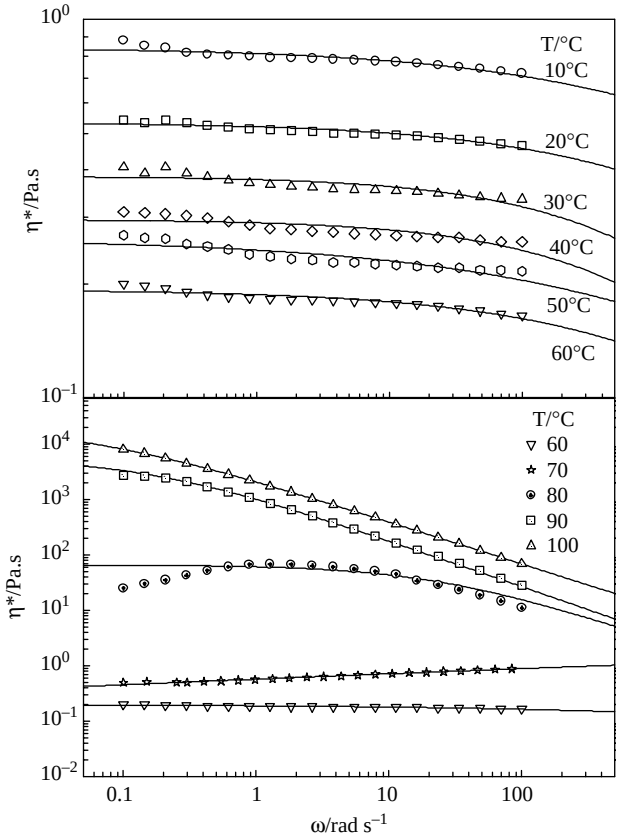

Fig. 7. Complex shear viscosity as a function of shear frequency at different temperatures for 40 wt% PU.

observed frequency dependence of dynamic viscosity can be well described by the following equation:

$$\eta^* = \frac{\eta_0}{1 + (\omega/\omega_c)^{\beta}} \quad (1)$$

where η_0 is the zero-shear viscosity, ω_c is the critical shear frequency value at which the viscosity decreases to half its initial value and β is a material constant that depends on the nature of the dispersion. Excellent description of the experimental data was obtained using this equation (cross model) as Fig. 7 shows, where the lines are fitting lines and the symbols are the experimental data. Table 2 shows the values of the fitting parameters obtained from the non-linear regression at different temperatures for 40 wt% PU. At a temperature range lower than the T_{gel} (i.e. $T \leq 60$ °C) the viscosity of the dispersion decreases gradually with increasing temperature. The viscosity increases strongly in the temperature range $T > T_{gel}$; for example, at 90 °C the viscosity is about four orders of magnitudes higher than its value at 60 °C. The viscosity decrease at 80 °C in the low frequency range is mainly due to a kinetic phenomenon because the gelation process evolves during the measurements; at high temperatures, particularly at the early stage of gelation process the viscosity increases dramatically. For example at 70 °C the viscosity increases slightly with increasing frequency which is contrary to the normal behavior (i.e. viscosity either constant or decrease with increasing shear frequency). At 80 °C the gelation process

Table 2
Viscoelastic parameters for 40% PU sample at different temperature obtained from Eq. (1)

T (°C)	η_0 (Pa·s)	ω_c (rad/s)	β
10	1.3	31,178	0.35
20	0.63	8079	0.4
30	0.31	826	0.8
40	0.27	2336	0.5
50	0.21	6352	0.8
60	0.17	614	0.4
70	0.66	35,071	0.3
80	65	1321	0.8
90	1000	1071	0.7
100	1700	3162	0.3

accelerated so much by the thermal energy and the viscosity increases during the measurement particularly at low frequency because of the relatively long residence time of the sample during the measurements under these conditions. Therefore, the viscosity starts with a small value at 0.1 rad/s and subsequently the viscosity increases with frequency (or with gelation time) up to a maximum value at 1 rad/s and then decrease again with frequency (Table 2).

The temperature dependence of η_0 obtained from fitting the data in Fig. 7 to Eq. (1) is shown in Fig. 8; obviously η_0 follows the same trend as that observed in the dynamic temperature ramps of G', G'' and η^* (Figs. 2–4), where there is a sudden change in sign of the slope (v-shape, Fig. 8) and an increase in η_0 with increasing T at T_{gel}. The arrow in Fig. 8 indicates the value of the T_{gel}, estimated from the intersection of the two different slopes of η_0 at different temperatures. This method gave a $T_{gel} = 68$ °C that is in good agreement with the value determined from tan δ versus T data (Fig. 5(a)).

The WLF, time–temperature–superposition principle can be used to construct master curves for the viscoelastic material functions based on thermorheological simplicity, i.e. any viscoelastic material function, f, can be superimposed by horizontal shifts along the x-axis (frequency axis):

$$f(\omega a_T, T_0) = f(\omega, T) \quad (2)$$

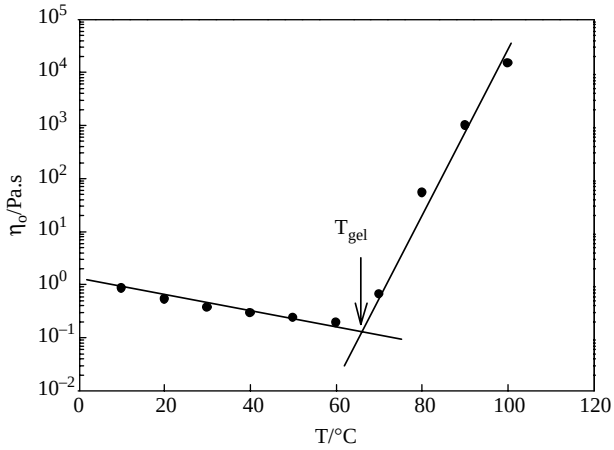

Fig. 8. Zero-shear viscosity as a function of temperature for 40 wt% PU. The array shows the value of T_{gel}.

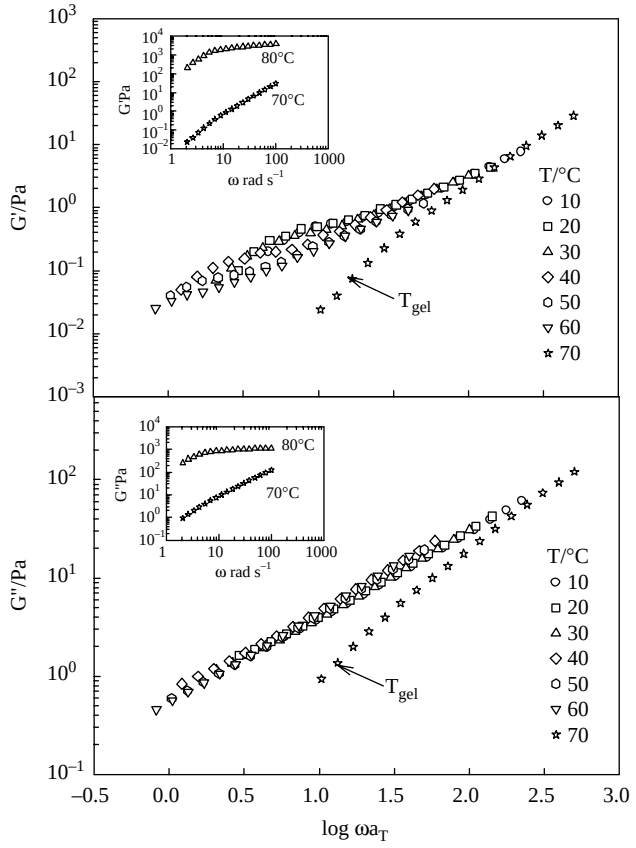

Fig. 9. Master curves of storage and loss moduli for 40 wt% PU at 30 °C.

where a_T is the horizontal shift factor and T_0 is the reference temperature. Fig. 9 shows the master curves of the dynamic shear moduli, G' and G'' for 40 wt% PU at $T_0 = 30$ °C. Obviously, we cannot construct only one master curve for the whole range of temperature due to the observed structure evolution in the system. The WLF principle is only valid for temperatures lower than the T_{gel}; the principle failed for $T \geq 70$ °C. This can be seen very clearly in the low frequency region as a deviation from the terminal slope in the G' and G'' curves. At $T \geq 80$ °C, G' and G'' cannot be plotted on the same master curve because they strongly increase by 2–3 orders of magnitude and G' exceeds G'', as shown in the inset plot of Fig. 9.

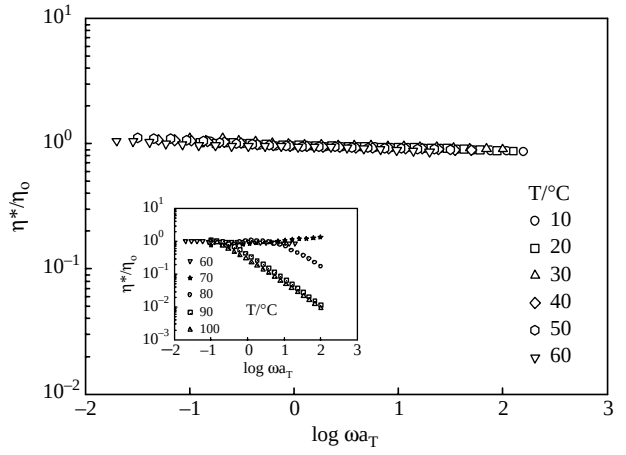

Fig. 10. Master curve of reduced viscosity η^*/η_0 for 40 wt% PU at 30 °C in a temperature range lower than T_{gel}. The inset plot shows the deviation of the master curve at $T \geq T_{gel}$.

Similar behavior can be obtained in the master curve of the dynamic shear viscosity as demonstrated in Fig. 10. At a temperature range higher than the T_{gel} the WLF is no longer applicable and a clear deviation from the master curve can be observed, as represented in the inset plot of Fig. 10. This deviation in the master curve is due to the influence of an excess viscosity caused by thermal-induced gelation and formation of fractal gel.

3.2. Morphological studies

Fives samples of different concentrations (i.e. 34, 36, 38, 40 and 42 wt%) were annealed in tightly closed glass bottles for 2 h at 70 °C in a water bath. All the samples changed to fractal gel except the 34 wt% PU which remained in the liquid state during the entire period of annealing time. The morphology of the different samples were examined using an optical microscope equipped with a CCD camera. Different morphologies were obtained as a function of concentration as shown in Fig. 11. A typical co-continuous structure with a unique periodicity and phase connectivity was observed for only 36, 38 and 40 wt% PU, and, no morphology was detected for 34 and 42 wt% PU. It is well known that a co-continuous structure such as the present one is a unique structure for mixtures that have undergone a phase separation via spinodal decomposition [46]. Therefore, the observation of co-continuous morphology indicates that these three samples were in the two-phase regime for a period of time long enough to allow the samples to phase separate via spinodal decomposition. Differences in the observed morphologies and phase separation depicted in Fig. 11 are ascribed to the different location of the samples in the phase diagram as well as the extent of the quenching depth of each sample. To support this hypothesis, a phase diagram is drawn schematically in Fig. 12. This phase diagram shows a liquid–liquid phase separation (LCST-type phase diagram) and a liquid–solid transition (gelation), both of them are located in the same temperature range, reflecting the complex behavior of the temperature effects on these PU dispersions. Based on this phase diagram it appears that a co-occurrence of liquid–liquid transition (phase separation) and liquid–solid transition (gelation) of aqueous PUDs can be induced thermally. The straight line with open circular symbols in Fig. 12 shows the location of the five samples in the phase diagram at 70 °C. The sample of 34 wt% PU is outside the liquid–liquid and liquid–solid transitions phase regions, therefore neither gelation nor phase separation morphology was detected for this composition at 70 °C. For the 42 wt% PU, it is outside the LCST-phase diagram but inside the liquid–solid phase diagram, therefore only gelation process can be observed (see for example Fig. 6(b)) without any phase separation morphology as shown in Fig. 11(e). The other three samples (i.e. 36, 38 and 40 wt%) are located inside both the LCST and the liquid–solid phase diagrams, therefore the two transitions

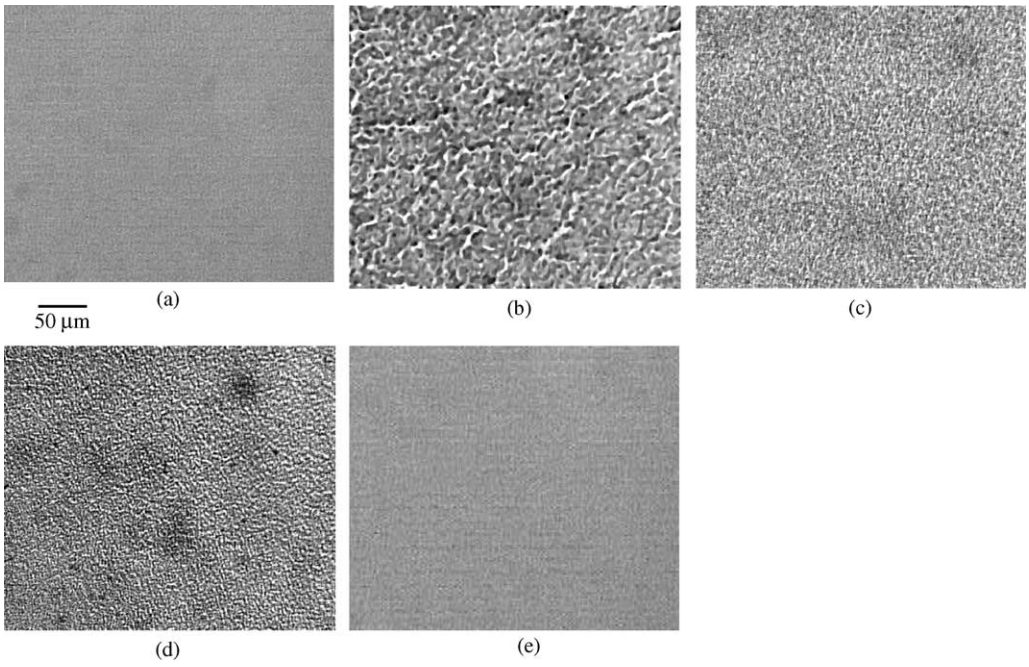

Fig. 11. Optical micrographs for five different PUDs after annealing in tightly closed glass bottles at 70 °C for 2 h in water bath: (a) 34 wt%; (b) 36 wt%; (c) 38 wt%; (d) 40 wt%; and (e) 42 wt% PU.

occur simultaneously at the same time. The reason for the observed different morphologies may be ascribed to the value of the quenching depth, ΔT, in the LCST-phase diagram; coarse morphology implies a large value of ΔT. This phase diagram (Fig. 12) shows that the value of ΔT decreases with increasing concentration for these three samples, therefore, the different morphologies of PUDs in Fig. 11 is not surprising at all.

It is very difficult to construct a real phase diagram for the complex PUD system of this study because of the simultaneous occurrence of the two transitions in the same temperature range. Based on the observed morphologies (Fig. 11), one can conjecture that the dramatic increase in the viscoelastic material functions of 40 wt% is not only caused by the gelation process but also by the contribution of the concentration fluctuations produced during the liquid–liquid phase separation. The simultaneous occurrence of liquid–liquid phase separation and gelation in this composition (40 wt% PU) makes the thermal behavior very complex and intriguing. However, only the gelation process was observed for the 42 wt%, implying that the temperature dependence of viscoelastic material functions of 42 wt% PU is typical of a classical gelation process. It is also important to note that the contribution of the concentration fluctuations to the viscoelastic material functions during the phase separation process is very little compared to the contribution of the very long relaxation times of the elastic gel [36]. Therefore, the gelation process is clearly responsible for the observed dramatic change in the viscoelastic behavior of the dispersions. This assertion is somewhat supported by our previous work on polymer blends where we detected a little change in the viscoelastic behavior of poly(methyl methacrylate)/poly(α-methyl styrene-*co*-acrylonitrile) blend (LCST-type phase diagram) in the vicinity of the phase separation temperatures [40].

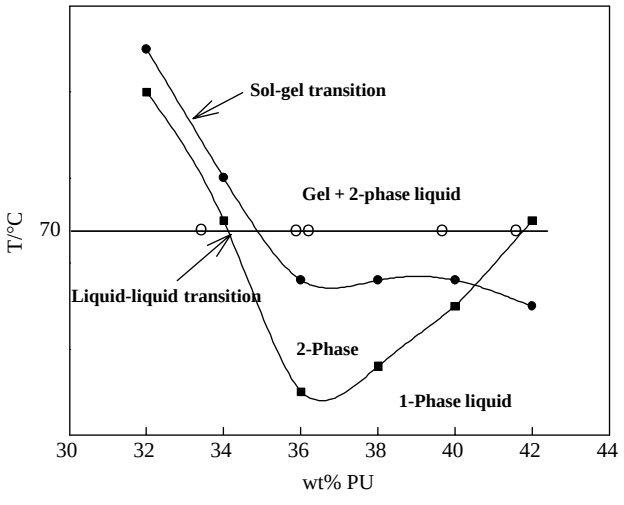

Fig. 12. Hypothetical Phase diagrams show a liquid–liquid phase separation and liquid–solid transition for PUDs. The straight line with open circular symbols shows the locations at 70 °C of the different five morphologies demonstrated in Fig. 11. Note that the 2-phase liquid indicated in the phase diagram is composed of both PU-rich and water-rich liquid phases of the dispersions as described in the text.

It is noteworthy that, a coexistence of phase separation and gelation process within a single composition ratio has been reported for a variety of water-soluble biopolymer aqueous solutions such as agarose, gelatin, fibrinogen and cellulose derivatives [41–45]. In these biopolymer solutions, the phase separation curve crosses the gelation curve in the concentration versus temperature phase diagram as in the present PUD case. Recently, thermal-induced coupling of phase separation and gelation in an aqueous solution of hydoxypropylmethyl cellulose (HPMC) has been reported by Kita et al. [45] who

used Fluorescence measurements on concentrated HPMC solution to confirm that the hydrophobic interaction is the driving force of gelation coupled by the phase separation [45].

The liquid–liquid and liquid–solid transitions can also simultaneously occur in charged colloidal dispersions [48]. The interparticle interaction for an aqueous charged colloidal dispersion was modeled by an effective hard-sphere Yukawa repulsion to which is added the long-range van der Waals attraction. The authors constructed the Helmholtz free energy and calculated the pressure and chemical potential needed in the determination of the liquid–liquid and liquid–solid coexistence curves. In addition, phase separation and gelation of polymer-dispersed liquid crystals has been studied theoretically and experimentally by Nakazawa et al. [49]. They studied the domain morphology resulting from phase separation by solving the coupled set of equations for the local volume fraction and the nematic order parameter, taking into account the viscoelastic effects and gelation due to polymerization [49]. In our case when the temperature approaches the gel point the viscosity increases strongly in a manner that is similar to the polymerization effect in the case of liquid crystal dispersions and consequently the phase separation takes place.

To our knowledge, the present study represents the first evidence of the occurrence of the above two transitions simultaneously in a single chemical composition of PUD, indicating a rich rheology/morphology behavior that is experimentally accessible, and for which the PUDs can serve as excellent model systems for studying the rheology and morphology evolution of this class of complex fluids. Very recently, Florez et al. investigated the rheological behavior of three different PU blocks in 2-butanone over a narrow range of temperature [47]. They found that annealing the clear solutions at around 0 °C resulted in thermoreversible gels that they attributed to crystallization of the soft segment (macroglycol) from the solution [47].

4. Conclusions

The viscoelastic properties of PUDs were investigated over a wide range of temperature and frequency for different compositions. Thermal-induced gelation were observed for PUDs with high concentration (PU wt% $\geq$ 36). During the dynamic temperature ramp experiments, an abrupt increase in the viscoelastic material functions (G', G'' and η^*) at the onset of gelation was observed at different angular frequencies. However, there was no tendency towards thermal-induced gelation for the low concentration samples (i.e. PU wt% $\leq$ 34). This finding is related to the difference in the particle sizes of the dispersions [34]; with increasing concentration, the PU particle size increases which in turn leads to increasing hydrodynamic interactions that can be increased by thermal energy and consequently leading to thermal-induced gelation. The gelation process for the 42 wt% PU sample takes place at lower temperature than that of 40 wt% PU. In addition, the high concentration of 42 wt% PU leads to an increase in the viscosity and a decrease in the dynamics of the particles, and consequently to a low probability for the particle–particle interaction. This is why the gelation process of 42 wt% PU starts at lower temperature but slower than that of 40 wt% PU. The gel-temperature, T_{gel}, could be determined from the temperature ramp of loss tangent, $\tan\delta$, at different shear frequencies, where all curves coincide regardless of the applied shear frequency. Similar values of T_{gel} (67 and 65 °C for 40 and 42 wt% PU, respectively) were determined from the crossover points of G' and G'' regardless of the different values of frequencies. The value of T_{gel} was also evaluated from the temperature dependence of zero-shear viscosity, η_0, and found to follow the same trend as that observed in the temperature ramps of G', G'' and η^* (i.e. a dramatic increase in η_0 is observed at T_{gel}). The morphology of the dispersions for some different PU concentrations showed a network structure with a unique periodicity and phase connectivity. Using the observed morphologies, we estimated an LCST-type phase diagram for these dispersions that was found to be consistent with the simultaneous occurrence of liquid–liquid and liquid–solid transitions at the same temperature range, like others have reported for other complex fluids such as biopolymer solutions. We hope that the results of the present study may stimulate a better understanding of the morphological changes in aqueous PUDs across the phase transition process.

Acknowledgements

This work was supported primarily by the MRSEC Program of the National Science Foundation under Award DMR 0213883. Partial support of this work from the Robert M. Hearin Support Foundation and Bayer Material Science, Pittsburgh, PA is gratefully acknowledged. We thank Anton Paar USA for providing us with direct access to their new MCR 501 rheometer. The anonymous reviewers are thanked for their insightful comments that improved the quality of the manuscript.

References

[1] Queslel JP, Mark JE. In: Allen G, editor. Comprehensive polymer science, vol. 2. Oxford: Pergamon Press; 1988. p. 271.
[2] Dušek K, Dušková-Smrčková M. Prog Polym Sci 2000;25:1215.
[3] Russel WB. Colloidal dispersions. New York: Cambridge University Press; 1989.
[4] van Megen W, Underwood SM. Phys Rev E 1994;49:4206.
[5] Pusey PN, van Megen W. Phys Rev Lett 1987;59:2083.
[6] Stiakakis E, Vlassopoulos D, Loppinet B, Roovers J, Meier G. Phys Rev E 2002;66:051804.
[7] Cates ME, Evans MR. Soft and Fragile Matter: Nonequilibrium Dynamics, Metastability and Flow: Proceedings of the Fifth Third Scottish University Summer School in Physics, St. Andrews, July 1999, Bristol, 2000.
[8] Segre PN, Prasad V, Schufield AB, Weitz DA. Phys Rev Lett 2001;86:6042.
[9] Chambon F, Winter HH. J Rheol 1987;31:683.
[10] Winter HH, Morganelli P, Chambon F. Macromolecules 1988;21:532.
[11] Scanlan JC, Winter HH. Macromolecules 1991;24:47.
[12] Izuka A, Winter HH, Hashimoto T. Macromolecules 1992;25:2422.
[13] Adolf D, Martin JE, Wilcoxon JP. Macromolecules 1990;23:527.
[14] Hodgson DF, Amis EJ. Macromolecules 1990;23:2512.

[15] Muller R, Gerard E, Dugand P, Rempp P, Gnanou Y. Macromolecules 1991;24:1321.
[16] Takahashi M, Yokoyama K, Masuda T, Takigawa T. J Chem Phys 1994; 101:798.
[17] Martin JE, Adolf D, Wilcoxon JP. Phys Rev A 1989;39:1325.
[18] Muthukumar M. J Chem Phys 1985;83:3162.
[19] Takigawa T, Takahashi M, Urayama K, Masuda T. Chem Phys Lett 1992; 195:509.
[20] Hess W, Vilgis TA, Winter HH. Macromolecules 1988;21:2536.
[21] Muthukumar M. Macromolecules 1989;22:4656.
[22] Lairez D, Adam M, Emer JR, Durand D. Macromolecules 1992;25:286.
[23] Adolf D, Martin JR. Macromolecules 1991;24:6721.
[24] Zhao Y, Cao Y, Yang Y, Wu C. Macromolecules 2003;36:855.
[25] Grisel M, Muller G. Macromolecules 1998;31:4277.
[26] Hone JH, Howe AM, Cosgrove T. Macromolecules 2000;33:1199.
[27] Balan C, Völger KW, Kroke E, Riedel R. Macromolecules 2000;33:3404.
[28] Daoud M. Macromolecules 2000;33:3019.
[29] Yoon PJ, Han CD. Macromolecules 2000;33:2171.
[30] Tanaka F. Macromolecules 1998;31:384.
[31] Matricardi P, Dentini M, Crescenzi V. Macromolecules 1993;26:4386.
[32] Stauffer D. Introduction to percolation theory. London: Taylor and Francis; 1985.
[33] De Gennes P-J. Scaling concepts in polymer physics. Ithaca: Cornell University Press; 1979.
[34] Schiessel H, Blument A. Macromolecules 1995;28:4013.
[35] Cross MM. J Colloid Sci 1965;20:417.
[36] Madbouly SA, Otaigbe JU, Nanda AK, Wicks DA. Macromolecules 2005;38:4014.
[37] Krieger IM, Dougherty TJ. Trans Soc Rheol III 1959;137.
[38] Madbouly SA, Ougizawa T. J Macromol Sci, Phys Ed 2004;B43:471.
[39] Zhao Y, Cao Y, Yang Y, Wu C. Macromolecules 2003;36:855.
[40] Madbouly SA, Ougizawa T. J Macromol Sci, Phys Ed 2002;B41:271.
[41] San Biagio PL, Bulone D, Emanuele A, Palma-Vittorelli MB, Palma MU. Food Hydrocolloids 1996;10:91.
[42] Tanaka T, Gerald S. Phys Rev Lett 1979;42:1556.
[43] Kaya M, Toyama Y, Yamada A, Sakanishi A, Kubota K. Trans MRS-J 2002;27:597.
[44] Takahashi M, Shimazaki M, Yamamoto J. J Polym Sci, Polym Phys Ed 2001;39:91.
[45] Kaya M, Kaku T, Ohashi H, Kurosu T, Iida M, Yagihara S, et al. Physica A 2003;319:56.
[46] Madbouly SA, Ougizawa T. Macromol Chem Phys 2004;205:979.
[47] Florez S, Munoz ME, Santamaría A. J Rheol 2005;49:313.
[48] Lai SK, Wu KL. Phys Rev E Stat, Nonlin, Soft Matter Phys 2002;66: 041403.
[49] Nakazawa H, Fujinami S, Motoyama M, Ohta T, Araki T, Tanaka H, et al. Comput Theor Polym Sci 2001;11:445.